Journal of Inorganic and General Chemistry
ZAAC
Zeitschrift für anorganische und allgemeine Chemie
www.zaac.wiley-vch.de
RESEARCH ARTICLE
Check for updates
DOI: 10.1002/zaac.202300106

Special Collection

$[Zr_6(\mu_3\text{-}O)_4(\mu_3\text{-}OH)_4](1\text{-adamantanecarboxylate})_{12}]$: a model for extrinsic "defect-engineerable" porosity

Vasily Gvilava,[a] Maximilian Vieten,[a] Tobias Heinen,[a] Robert Oestreich,[a] Ishtvan Boldog,*[a] and Christoph Janiak*[a]

Dedicated to Prof. Dr. Michael Ruck on the occasion of his 60th Birthday.

The molecular zirconium-oxo cluster with 1-adamantanecarboxylate of ideal formula $[Zr_6O_4(OH)_4(AdCA)_{12}]$ (AdCA = 1-adamantanecarboxylate) has a near spherical shape with a hydrophobic "shell" of bulky rigid adamantyl groups. The use of formic acid as a modulator and a large excess of the HAdCA were found to be crucial for its reproducible synthesis and the formation of ~100-150 µm well-formed rhombohedral single crystals. Crystallization in the presence of formic acid leads, however, to ligand-substitution defects (1-2 out of 12) which were quantified by thermogravimetry and NMR. A defect-engineering with a higher defect ratio in such oxo clusters is a promising approach aiming at extrinsic porosity.

Introduction

Metal-oxo clusters (MOCs) are a well-established class of molecular compounds, including polyoxometalates (POM) as the largest and most important sub-set.[1] The multinuclear coordination-bonded core of MOCs, mainly by group IV–VI metals, is typically constituted by M–O-M bridges, involving O^{2-}, OH^- and H_2O ligands. The outer shell is stabilized by terminal/capping ligands, both inorganic (e.g. sulfate or peroxide) or organic ones.[2,3] A class of compounds, interesting in the context of this contribution, is the metal-oxo carboxylate clusters with a general formula of $[M_xO_y(RO)_z(H_2O)_u(R'COO)_w]$ (R, R' = H, alkyl, aryl, *etc.*). The MOCs represent nanoobjects with defined structure and true solubility unlike most nanoparticles, which are characterized by a certain size distribution and which form colloidal solutions.[4]

Zr^{4+} ions, typically eight-coordinated have a particular propensity to form zirconium-oxo clusters, ZrOCs in the presence of carboxylates. The dominant self-assembly route leads to $\{Zr_6\}$ clusters such as $[Zr_6O_4(OH)_4(RCOO)_{12}]$ (Figure 1a), even if various other ZrOCs, for example $\{Zr_3\}$,[5] $\{Zr_5\}$,[6] $\{Zr_4\}$,[7,8] $\{Zr_{10}\}$,[9] $\{Zr_{18}\}$,[10] $\{Zr_{26}\}$[11] and even $\{Zr_{70}\}$ (with sulfate as a co-ligand) also could form.[2] ZrOCs have been actively developed primarily by Kickelbick and Schubert,[4,5,7–9,12,13] and still offer interesting novelties.[2]

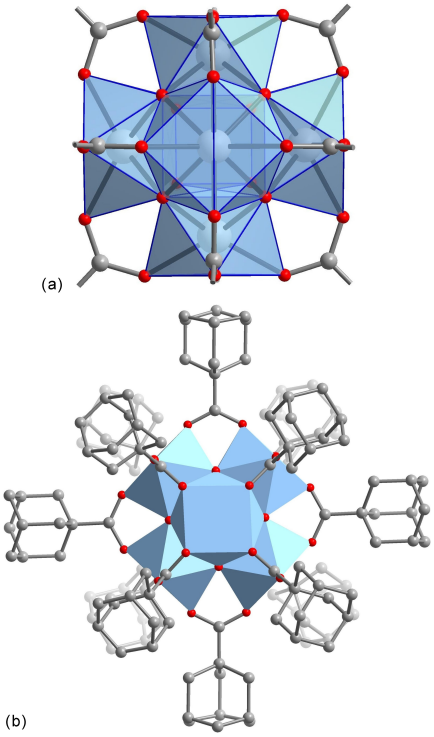

Figure 1. The structure of the paradigmatic $[Zr_6O_4(OH)_4(RCOO)_{12}]$ cluster: (a) isolated; (b) as a part of $[Zr_6O_4(OH)_4(AdCA)_{12}]$, **1** (AdCA = 1-adamantanecarboxylate). The disorder of AdCA and the hydrogen atoms are not shown for clarity.

[a] *V. Gvilava, M. Vieten, T. Heinen, R. Oestreich, I. Boldog, Prof. C. Janiak*
Institut für Anorganische Chemie und Strukturchemie
Heinrich-Heine-Universität Düsseldorf
40204 Düsseldorf, Germany
E-mail: ishtvan.boldog@gmail.com
janiak@uni-duesseldorf.de

Supporting information for this article is available on the WWW under https://doi.org/10.1002/zaac.202300106

This article is part of a Special Collection dedicated to Professor Michael Ruck on the occasion of his 60th birthday. Please see our homepage for more articles in the collection.

Importantly, the ZrOCs could be viewed as building blocks for hybrid materials, such as cluster-crosslinked polymers[4,14] metal-organic gels,[15] photocatalytic materials[16] and metal-organic frameworks (MOFs).[17] The latter are crystalline porous materials that typically possess three-dimensional network structures with potentially permanent porosity.[18] For the zirconium MOFs the cluster concept is fundamental, since the majority of them such as UiO-66,[19] MOF-808,[20,21] and NU-1000[22] are typically build up from geometrically regular metal clusters identical to ZrOCs, interconnected by oligocarboxylate ligands.[23,24] Therefore, ZrOCs could be even used as precursors for MOF synthesis due to the possibility of post-synthetic carboxylate-ligand exchange, as demonstrated in $[Zr_6O_4(OH)_4(OMc)_{12}]$ (OMc = methacrylate).[23,25] A particularly important feature of Zr-MOFs is their inclination to form defects,[26] the most typical of which are associated with the variation of the ligand completing the ZrOCs, allowing thereby variations of the available free volume/surface and chemical properties (particularly the Lewis acidity).[27,28]

However, there are other subtle means inspired by defective MOFs, by which ZrOCs as discrete molecules could, potentially, be used for sustaining porosity. On the one hand, the packing efficiency of large discrete molecules depends on the shape of the molecules, while the size of intermolecular voids increases with the size of the molecules (*cf.* with the close packing of equally-sized spheres with the highest packing density of ~74% for both the optimal *fcc* or *hcp* cases). There are molecular shapes possessing a combination of geometric features (with symmetry as one of the important distinct descriptor) – e.g. triptycene-based molecules[29] – which commands particularly low packing efficiencies. The residual porosity, associated with non-tight packing is often referred to as "extrinsic" porosity, which could be contraposed to "intrinsic" porosity, i.e. inherent "interior" porosity.[30] On the other hand, the propensity of ZrOCs to express ligand defects, or, potentially, allow their generation postsynthetically (i.e. by partial decomposition or elimination of the capping ligands, with the latter case well-documented for MOFs[28]) gives a particular way to decrease the packing efficiency, i.e. generate larger porosity.

There are two recognized prerequisites, which increase the chances of employing ZrOCs for creating permanently porous supramolecular materials sustained only by weak non-covalent interactions. Firstly, it is necessary to reach a sufficiently large size of the molecular ZrOC units to reach the limits of a contiguous accessible pore system allowing the evacuation of the guest molecules (even if relatively small molecules could sustain extrinsic porosity, see e.g. $[Zn_4(\mu_3\text{-}OH)_2(L)_4(tBuO)_2]$,[31] larger size is beneficial). Secondly, the possibility to create defects (primarily understood as random substitution of bulkier regular ligands by smaller ones),[28] which could be used for porosity tuning. The structures of $[Zr_6O_4(OH)_4(OOCR)_8(H_2O)_8]^{4+}$ and $[Zr_5(O)_2(OH)_6(OOCR)_4(H_2O)_{11}(alcohol)]^{6+}$ are examples for the removal of not only the carboxylate ligands but also of the metal ions to create defects.[6] In this regard, ZrOCs are interesting models for "inorganic-core" dendrimers, with the advantage of straightforward crystallization of geometrically regular molecules and yet with a level of tuneable local irregularity, also possible for (the generally more geometrically flexible) classical dendrimers. The latter, which are highly branched polymeric macromolecules, could demonstrate extrinsic porosity, however, usually, the interpenetration of the 'dendron' branches of structurally irregular and often flexible molecules represent a packing opportunity detrimental to the realization of micropores.[32–34]

In order to demonstrate the potential of ZrOCs for the realization of extrinsic porosity enhanced by "defect-engineering", bulky rigid ligands are deemed to be preferable, at least on the level of proof-of-concept. Such ligands provide an approximation towards a rigid spherical shape with minimized "indents", which could ensure an approximation of a sphere packing. Additionally, the steric repulsion of the ligands might stimulate the formation of defects (i.e. *via* substitution by a smaller ligand). For the $[Zr_6O_4(OH)_4(RCO_2)_{12}]$ cluster in molecular form, the relatively bulky cases of $R = C(CH_3)_3$ and $C(CH_3)_2Et$ were reported by Piszczek *et al.*[35] Yet, Zr-MOFs with bulky ligands are not numerous. UiO-66 analogs with relatively small cage-based bridging ligands were reported with bicyclo[1.1.1]pentane-1,3-dicarboxylate[36] and bicyclo[2.2.2]octane-1,4-dicarboxylate (NU-403).[37] Recently, we have reported the bulky 4,9-adamantanedicarboxylate-based analogue (HHUD-3),[38] which shows porosity only due to the presence of defects.

In this contribution, we report the structure and properties of the new molecular ZrOC $[Zr_6O_4(OH)_4(AdCA)_{12}]$ (Figure 1b) (AdCA = 1-adamantanecarboxylate) to make the step towards the yet unexplored possibility to create extrinsically porous crystalline solids with "defect-engineering", although at present this is a conceptual proof-of-concept of a possibility rather than a final result.

Results and Discussion

The synthesis of $[Zr_6O_4(OH)_4(AdCA)_{12}]$, yielding a crystalline solid composed of ~100–150 μm single crystals (Figure S1, Supp. Info.) was carried out under low-temperature solvothermal synthesis ($ZrOCl_2 \cdot 8H_2O$:HAdCA:DMF:HCOOH at ~1:60:750:40 ratio, 120 °C; see Supp. Info. 1). The use of formic acid and a very large excess of the HAdCA, which could be viewed as a modulator and self-(co)-modulator, respectively, were found to be crucial (see[39–40] for the role of modulators in enhancing crystallinity and affecting the crystal sizes). Importantly, a smaller excess of 1-adamantanecarboxylic acid could lead to another unidentified crystalline phase (Supp. Info. 3), while smaller batches (~30 mg) yielded a product with lessened crystal co-growth and, hence, undesired solvent occlusion (combined products of parallel small batch syntheses were used for analytics).

The single crystal X-ray diffraction (SCXRD) structure confirms the expected $[Zr_6(\mu_3\text{-}O)_4(\mu_3\text{-}OH)_4(AdCA)_{12}]$ structure of **1** ($R\bar{3}$, $a = 25.202$ Å; Supp. Info. 2). The six metal ions are located at the vertices of an octahedron with the eight triangular faces capped by crystallographically site-sharing μ_3-O/OH groups, which are face-alternating in an isolated cluster. With the

average distance between Zr^{4+} ions of 3.51 Å it is similar to the reported clusters $[Zr_6O_4(OH)_4(OMc)_{12}]$ (OMc = methacrylate),[41] $[Zr_6O_4(OH)_4(O_2CBu^t)_{12}]$[35] as well as the Zr-clusters of the standard UiO-66 type MOFs.[42] There are two symmetry-independent 1-adamantanecarboxylates, which are propagated by the $\bar{3}$ axis to constitute the 6 + 6 intra-bridging ligand set of the cluster, which correspond to the twelve edges of the octahedron. As a result, each Zr^{4+} ion is surrounded by four oxygen atoms of the carboxylic groups (Zr–O distances of 2.190(3)-2.244(3) Å correspond to literature values[42]) and four μ_3-O or μ_3-OH groups in a square antiprism. The μ_3-O atoms of the oxido- and hydroxido- ligands are located 0.36 and 0.99 Å away from the Zr_3 planes, respectively.

The inorganic core of the cluster is shielded by a surrounding layer of non-polar adamantyl moieties. This results in a structure, which can be approximated as a sphere with a vdW diameter of ~21.5 Å (Figure 2). The dimples/indentions on the surface of the sphere, associated with the inter-ligand space as well as with the profile of the outer face of the adamantyl group, namely the cyclohexane moiety in a fixed chair conformation, cause a denser packing ($\varrho = 1.467\ g\,cm^{-3}$) than one might expect. The small void spaces (Figure 3a), that are inaccessible to solvents, make up for less than 1% of the unit cell. The latter consists of a total of 3 clusters: 2 complete, 2×1/3 clusters, and 2×1/6 clusters (Figure 3b); the packing of the clusters corresponds to *hcp* type (Figure 3c). The isolated pockets would only be enough to host water molecules (but not nitrogen), and the respective surface area is calculated to be ~82 $m^2\,g^{-1}$ (2.4 Å probe diameter, Table S4, Supp. Info. 11).

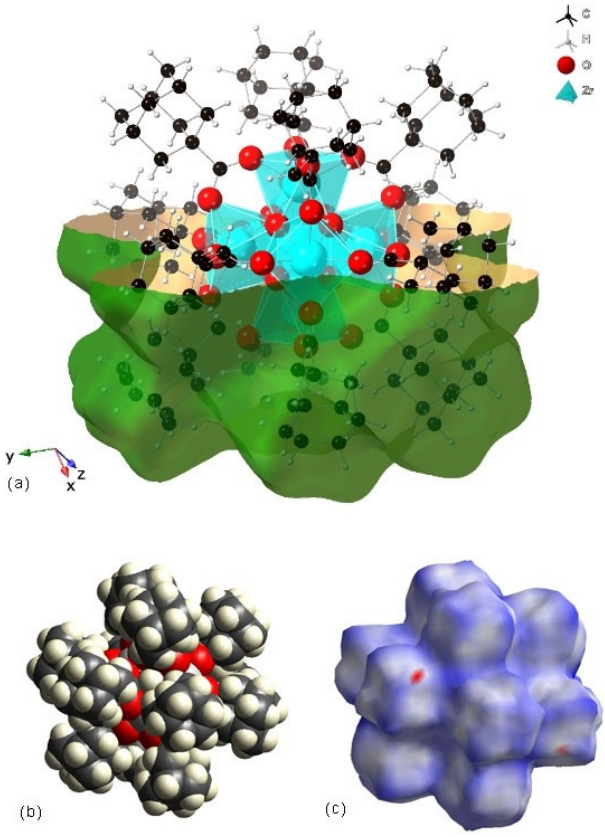

Figure 2. Views of the $[Zr_6(\mu_3\text{-}O)_4(\mu_3\text{-}OH)_4(AdCA)_{12}]$ molecular cluster: (a) ball and stick representation with half of the vdW surface; (b) space-filling representation; (c) Hirshfeld isosurface (w(r) = 0.5) with the white color mapping corresponding to near equal-, blue to longer-, and red to shorter sum of atom-to-surface contact distances than the sum of the atom's vdW radii.

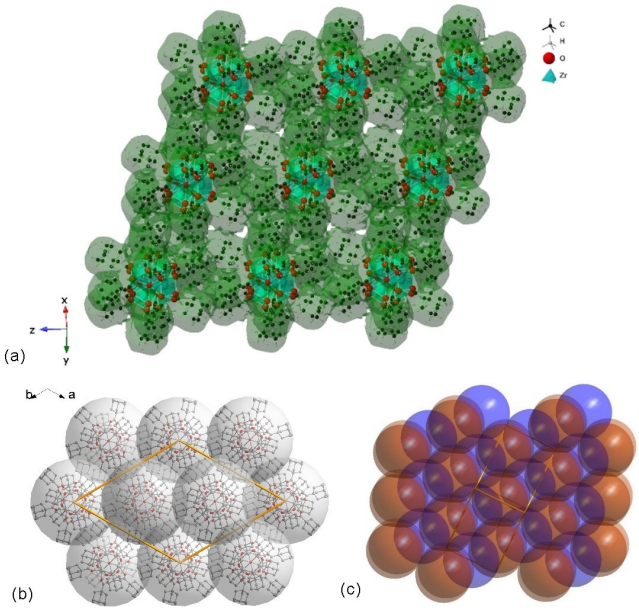

Figure 3. Molecular packing in the structure of **1**: (a) a thin slice revealing the residual unoccupied volume; (b) disposition of the molecular units in the unit cell; (c) *hcp* packing of the molecules (ABAB…, the A and B layers are given in different colors).

The molecules of **1** are stable in the solution. They could be observed by DLS (Supp. Info. 8), even if on the verge of the capabilities of the method and are stable enough to retain their hexanuclear nature under MALDI-TOF conditions, even if ligand exchange does occur (Supp. Info. 9). Interestingly, **1** is poorly soluble, which correlates with the observed energetically favorable tight packing. Despite the hydrophobic structure of the cluster, the solubility tests even in common hydrophobic solvents showed unexpectedly poor results, with the best solubility in chloroform (3.6 $g\,L^{-1}$), followed by dichloromethane (1.4 $g\,L^{-1}$, Supp. Info. 7). The low solubility could be viewed as a result of the aggregate action of a multitude of CH···HC dispersion interactions, sometimes referred to as "sticky fingers" (the effect is created by the number and not specifically strong interactions; the Hirshfeld surface shows almost no strong interactions (Figure 2c). This might be also the reason of the apparently slow crystallization kinetics).[43]

The focal point of interest for us is whether the cluster has defects, as it could prove the possibility of defect-driven porosity tuning for ZrOC-based molecular solids. While elemental analysis is imprecise here, as the defects might be filled by trapped solvent molecules, thermogravimetric analysis (TGA) is a valuable tool in this regard (Fig. S8, Supp. Info. 6). A two-step weight loss was registered: 6.1% from r.t. to ~330 °C due to

"dehydroxylation" (i.e. dehydration) and (minor) possible loss of the occluded mother solvent, as well as ~65% weight loss from ~330 to ~600 °C due to the decomposition/oxidation of the organic ligands, leaving ~29% of residual ZrO_2. Based on the TGA data, 2.2 'missing' AdCA ligands out of 12 per cluster are estimated, which are assumed to be near-exclusively substituted by formate ions, as the alternative 'defect-termination' by OH^-/H_2O is less favorable in the presence of formic acid (the influence on the assignment on the TGA is negligible, particularly compared to the potential impact of the occluded solvent).

The IR evidence for the formate presence is unconvincing as the CH stretching vibration of formate (2800–2900 cm^{-1}) overlaps with the vibrations of the adamantyl CH_2 and CH groups (Supp. Info. 5), while the CH bending vibration of formate (1400 cm^{-1}) overlaps with a stronger symmetric stretching vibration of the AdCA carboxylate group. However, the IR spectroscopy evidences the purity of the product (see Supp. Info. 5 for the assignments), as well the low amount of occluded solvent (the characteristic peaks for the non-coordinated carboxylate of the free ligand at ~1700 cm^{-1} and the amide of the DMF at ~1650 cm^{-1} are practically absent).

^{1}H NMR, despite relatively low sensitivity, is better suited for the detection of formate. The actual spectrum of **1** in $CDCl_3$ (Supp. Info. 4) unequivocally shows the presence of 1-adamantanecarboxylate and no free acid (which confirms the expected stability of the compound in the solution). However, the poor solubility of the compound in all tested solvents necessitates the digestion of the sample for better determination of the minor formate. The digested sample in $DCl/D_2O/THF\text{-}d_8$ indicates the presence of formic acid (FA), with a FA:HAdCA ratio of ~1:11.8, or 0.94 defects out of 12 ligands (the ratio is already corrected for the presence of occluded mother solvent, which is derived from the DMF content; see Supp. Info. 4. It is also worth noting the near absence of $Me_2NH_2^+$, which confirms that no formic acid comes from the hydrolysis of DMF).

Finally, the SCXRD analysis also indicates the presence of defects, but to a minor extent: free refinement of the occupancy of the ligands gives only 0.29 defects. It is important to note that the method is not precise in this regard. One of the significant error sources is due to the disorder in one of the two independent AdCA ligands, which results in relatively higher total occupancy under free refinement (which could be explained as an excessive account of "background" residual electronic densities), revealing practically no defects for this particular moiety. However, for the non-disordered ligand, the refined occupancy is ~0.95, which is more realistic and represents 0.6 defects out of 12 ligands. Despite significant discrepancy by different methods, the two more reliable methods give a number of ~1 or more defects out of 12.

The measured N_2-based surface area of the crystallized and activated **1** is nearly non-existent. However, extrinsic porosity is possible for large molecular Zr-clusters as was shown with one of the largest known zirconium cluster with an idealized formula of $[Zr_{26}O_{18}(OH)_{30}(HCOO)_{38}]$ which was obtained by the solvolysis of $ZrOCl_2$ in DMF/HCOOH.[11] Supercritical CO_2 drying followed by degassing at 190 °C yielded a surface area $S_{BET} \approx 146\ m^2 g^{-1}$ from the nitrogen sorption isotherm. The desorption branch featured an H2-type hysteresis, which is characteristic for mesoporous solids with 'ink-bottle' pores. The activated material adsorbed 0.55 mmol g^{-1} of CO_2 at 273 K and 0.25 wt% of H_2 at 1 bar and 77 K, which matched the expected values for the calculated surface area.[11] The presence of small, albeit evident extrinsic porosity in the $\{Zr_{26}\}$ cluster suggests that it is the size what matters, hence our approach to bring large ligands onto the more common $\{Zr_6\}$ cluster.

The attempt to form a crystalline film by evaporation of a solution of **1** in CH_2Cl_2 failed, even if the evaporation was done slowly. Obviously, one or even two defects are themselves still not enough to provide a contiguous pore system (for a model with two ordered ligand defects the surface area of the inaccessible pores should be ~170 $m^2 g^{-1}$ for N_2 sized molecules, Table S4, Supp. Info. 11). However, more defects and non-regular packing could drastically increase the accessible surface area, even if supramolecular structures might also, at least partially, adapt their packing to fill the empty space. At the same time, the synthesis of large defected $\{Zr_6\}$ molecular clusters is shown here to be a viable 'design' approach.

Conclusions

In summary, the successful synthesis of $[Zr_6O_4(OH)_4(AdCA)_{12}]$, a large near-spherical molecule with shell of bulky organic ligands, demonstrates an interesting approach to create large 'dendrimer-like' objects, yet of a high level of order and crystallizable due to the reversibility of the core-formation and its precise geometric definition. The presence of an appreciable amount of ligand defects (formates instead of adamantanecarboxylates) was demonstrated, which is interesting in the context of zirconium-oxo cluster-based 'extrinsically' porous solids with a possibility of porosity tuning via 'defect-engineering'. Yet, the tuning of the number of defects needs a refined control over the crystallization process. However, the presented results offer an optimistic view toward this type of porosity, which is associated with soluble molecular precursors and their extrinsic porosity created upon deposition, e.g., in thin films. The positive outlook is also due to easy post-synthetic ligand exchange for defect tuning in ZrOCs, even if the products might not be easily crystallizable.

Experimental Section

Materials and Methods

All chemicals were used as received from the suppliers (see section 1, in the Supp. Info.).

For the single crystal X-ray diffraction structure determination (SCXRD) a suitable transparent crystal of **1** was mounted on a microloop in a drop of immersion oil. The measurement was performed using a XtaLAB Synergy (Rigaku) single crystal diffractometer equipped with a PhotonJet microfocus sealed tube X-ray source (Cu–Kα, λ = 1.54184 Å) at 100 K under nitrogen gas stream

(Oxford Cryostream liquid nitrogen cooling system). The data collection, calculation, data reduction, and adsorption correction were performed using CrysAlis PRO.[44] The structure was solved by SHELX-2018[45] and refined using Olex.[46] The hydrogen atoms were placed geometrically and refined with Uiso(H) = 1.2 Ueq(C) and Uiso(O) = 1.5Ueq(O) thermal displacement parameters regarding the respective parent atoms.

Powder X-ray diffraction (PXRD) patterns were measured over the 2θ range of 5–50° in reflective mode using a Rigaku MiniFlex600 and graphite monochromated Cu–Kα irradiation (λ = 1.54182 Å) at room temperature. The Rigaku MiniFlex600 diffractometer was operated using a 600 W source (40 kV, 15 mA) and equipped with a HyPix-400 MF 2D hybrid pixel array detector (HPAD); the measurements were performed with a 0.01° step. The Bruker D2 Phaser diffractometer was operated with a 300 W source (30 kV, 10 mA) and equipped with a Lynxeye 1D detector.

Brunauer-Emmett-Teller surface areas (S_{BET}) were determined by nitrogen (purity 99.999%, 5.0) sorption experiments at 77 K using liquid nitrogen cooling on a BELSORP MAXII instrument (BEL instruments, Japan) within a partial pressure range of $10^{-6} < pp_0^{-1} < 1$. The samples were degassed under vacuum ($p < 10^{-6}$ mbar) at 80 °C for ca. 8 h, prior to measurement.

Matrix-assisted laser desorption ionization time-of-flight (MALDI-TOF) mass spectrometry (MS) was performed using an UltrafleXtreme by Bruker Daltonic mass spectrometer (Bremen, Germany) in reflector mode at positive polarity. *Trans*-2-[3-(4-tert-butylphenyl)-2-methyl-2-propenylidene]malononitrile (DCTB) was used as matrix for the experiments with a sample-matrix mixture of 10 parts matrix and 1 part analyte.

Dynamic light scattering (DLS) was performed using a Malvern Nano S Zetasizer (He–Ne laser) (Malvern Panalytical GmbH, Kassel, Germany).The thermogravimetric analysis (TGA) was carried out on a Netzsch TG 209 F3 Tarsus instrument (NETZSCH-Gerätebau GmbH, Selb, Germany) with an aluminum oxide sample holder at a 5 °K min^{-1} heating rate under a synthetic air atmosphere (80% N_2/20% O_2) at a 10 mL min^{-1} flow. Infrared (IR) spectra were collected by a Bruker Tensor 37 FT-IR device (Bruker AXS, Karlsruhe, Germany) on samples distributed in a KBr matrix in the range of 4000–400 cm^{-1}. The solution ^{1}H NMR spectra were recorded at 300 MHz and 600 MHz using a Bruker Avance III instrument. Scanning electron microscopy (SEM) images were recorded on a Zeiss CrossBeam 550 (FIB-SEM) electron microscope (Carl Zeiss Microscopy, Germany).

Acknowledgements

The Rigaku X-ray diffractometer was funded by the Deutsche Forschungsgemeinschaft, DFG through grant 440366605. Open Access funding enabled and organized by Projekt DEAL.

Conflict of Interest

The authors declare no conflict of interest.

Data Availability Statement

The data that support the findings of this study are available from the corresponding author upon reasonable request.

Keywords: Defect-engineering · Zirconium-oxo cluster · Adamantane · Extrinsic porosity · Bulky ligands

[1] M. Nyman in *Polyoxometalates and Other Metal-Oxo Clusters in Nature* in *Encyclopedia of Geochemistry: A Comprehensive Reference Source on the Chemistry of the Earth* (Ed. W. M. White), Springer International Publishing, Cham, **2018**, pp. 1242–1247.
[2] Y. Zhang, F. De Azambuja, T. N. Parac-Vogt, *Coord. Chem. Rev.* **2021**, *438*, 213886.
[3] S. Gross, *J. Mater. Chem.* **2011**, *21*, 15853–15861.
[4] U. Schubert, *Chem. Soc. Rev.* **2011**, *40*, 575–582.
[5] B. Moraru, S. Gross, G. Kickelbick, G. Trimmel, U. Schubert, *Monatsh. Chem.* **2001**, *132*, 993–999.
[6] J. Pascual-Colino, B. Artetxe, G. Beobide, O. Castillo, M. Luz Fidalgo-Mayo, A. Isla-López, A. Luque, S. Mena-Gutiérrez, S. Pérez-Yáñez, *Inorg. Chem.* **2022**, *61*, 4842–4851.
[7] G. Trimmel, S. Gross, G. Kickelbick, U. Schubert, *Appl. Organomet. Chem.* **2001**, *15* 401–406.
[8] G. Kickelbick, M. P. Feth, H. Bertagnolli, M. Puchberger, D. Holzinger, S. Gross, *J. Chem. Soc. Dalton Trans.* **2002**, 3892–3898.
[9] G. Kickelbick, U. Schubert, *J. Chem. Soc. Dalton Trans.* **1999**, 1301–1306.
[10] T. Xu, X. Hou, Y. Wang, J. Zhang, J. Zhang, B. Liu, *Dalton Trans.* **2017**, *46*, 10185–10188.
[11] B. Nateghi, I. Boldog, K. V. Domasevitch, C. Janiak, *CrystEngComm* **2018**, *20*, 5132–5136.
[12] G. Kickelbick, P. Wiede, U. Schubert, *Inorg. Chim. Acta* **1999**, *284*, 1–7.
[13] M. Puchberger, F. R. Kogler, M. Jupa, S. Gross, H. Fric, G. Kickelbick, U. Schubert, *Eur. J. Inorg. Chem.* **2006**, 3283–3293.
[14] G. Trimmel, P. Fratzl, U. Schubert, *Chem. Mater.* **2000**, *12*, 602–604.
[15] J. Santos-Lorenzo, R. San José-Velado, J. Albo, G. Beobide, P. Castaño, O. Castillo, A. Luque, S. Pérez-Yáñez, *Microporous Mesoporous Mater.* **2019**, *284*, 128–132.
[16] J. Napal, B. Artetxe, G. Beobide, O. Castillo, A. Luque, J. Pascual-Colino, S. Pérez-Yáñez, M. Perfecto-Irigaray, *Inorg. Chem. Front.* **2022**, *9*, 935–940.
[17] Y. Bai, Y. Dou, L.-H. Xie, W. Rutledge, J.-R. Li, H.-C. Zhou, *Chem. Soc. Rev.* **2016**, *45*, 2327–2367.
[18] B. Li, H. M. Wen, Y. Cui, W. Zhou, G. Qian, B. Chen, *Adv. Mater.* **2016**, *28*, 8819–8860.
[19] J. H. Cavka, S. Jakobsen, U. Olsbye, N. Guillou, C. Lamberti, S. Bordiga, K. P. Lillerud, *J. Am. Chem. Soc.* **2008**, *130*, 13850–13851.
[20] H. Furukawa, F. Gándara, Y. B. Zhang, J. Jiang, W. L. Queen, M. R. Hudson, O. M. Yaghi, *J. Am. Chem. Soc.* **2014**, *136*, 4369–4381.
[21] J. Baek, B. Rungtaweevoranit, X. Pei, M. Park, S. C. Fakra, Y. S. Liu, R. Matheu, S. A. Alshmimri, S. Alshehri, C. A. Trickett, G. A. Somorjai, O. M. Yaghi, *J. Am. Chem. Soc.* **2018**, *140*, 18208–18216.
[22] T. Islamoglu, K.-i. Otake, P. Li, C. T. Buru, A. W. Peters, I. Akpinar, S. J. Garibay, O. K. Farha, *CrystEngComm* **2018**, *20*, 5913–5918.
[23] V. Guillerm, S. Gross, C. Serre, T. Devic, M. Bauer, G. Férey, *Chem. Commun.* **2010**, *46*, 767–769.
[24] A. A. Bezrukov, K. W. Tornroos, E. Le Roux, P. D. C. Dietzel, *Chem. Commun.* **2018**, *54*, 2735–2738.
[25] F. R. Kogler, M. Jupa, M. Puchberger, U. Schubert, *J. Mater. Chem.* **2004**, *14*, 3133–3138.
[26] G. C. Shearer, S. Chavan, J. Ethiraj, J. G. Vitillo, S. Svelle, U. Olsbye, C. Lamberti, S. Bordiga, K. P. Lillerud, *Chem. Mater.* **2014**, *26*, 4068–4071.

[27] S. Øien, D. Wragg, H. Reinsch, S. Svelle, S. Bordiga, C. Lamberti, K. P. Lillerud, *Cryst. Growth Des.* **2014**, *14*, 5370–5372.
[28] M. Taddei, *Coord. Chem. Rev.* **2017**, *343*, 1–24.
[29] D. Reinhard, W. S. Zhang, F. Rominger, R. Curticean, I. Wacker, R. R. Schroder, M. Mastalerz, *Eur. J. Chem.* **2018**, *24*, 11433–11437.
[30] D. Holden, S. Y. Chong, L. Chen, K. E. Jelfs, T. Hasell, A. I. Cooper, *Chem. Sci.* **2016**, *7*, 4875–4879.
[31] K. Sokolowski, W. Bury, I. Justyniak, D. Fairen-Jimenez, K. Soltys, D. Prochowicz, S. Yang, M. Schröder, J. Lewinski, *Angew. Chem. Int. Ed.* **2013**, *52*, 13414–13418.
[32] O. Serenko, K. Skupov, A. Bakirov, N. Kuchkina, Z. Shifrina, A. Muzafarov, *Nanomaterials* **2021**, *11*, 2600.
[33] O. Serenko, P. Strashnov, G. Kapustin, M. Kalinin, N. Kuchkina, E. Serkova, Z. Shifrina, A. Muzafarova, *RSC Adv.* **2017**, *7*, 7870–7875.
[34] C.-H. Lee, M.-R. Tsai, Y.-T. Chang, L.-L. Lai, K.-L. Lu, K.-L. Cheng, *Chem. Eur. J.* **2013**, *19*, 10573–10579.
[35] P. Piszczek, A. Radtke, A. Grodzicki, A. Wojtczak, J. Chojnacki, *Polyhedron* **2007**, *26*, 679–685.
[36] J. Perego, S. Bracco, M. Negroni, C. X. Bezuidenhout, G. Prando, P. Carretta, A. Comotti, P. Sozzani, *Nat. Chem.* **2020**, *12*, 845–851.
[37] K. B. Idrees, Z. Chen, X. Zhang, M. R. Mian, R. J. Drout, T. Islamoglu, O. K. Farha, *Chem. Mater.* **2020**, *32*, 3776–3782.
[38] V. Gvilava, M. Vieten, R. Oestreich, D. Woschko, M. Steinert, I. Boldog, R. Bulánek, N. A. Fokina, P. R. Schreiner, C. Janiak, *CrystEngComm* **2022**, *24*, 7530–7534.
[39] W. Morris, S. Wang, D. Cho, E. Auyeung, P. Li, O. K. Farha, C. A. Mirkin, *ACS Appl. Mater. Interfaces* **2017**, *9*, 33413–33418.
[40] G. C. Shearer, S. Chavan, S. Bordiga, S. Svelle, U. Olsbye, K. P. Lillerud, *Chem. Mater.* **2016**, *28*, 3749–3761.
[41] G. Kickelbick, U. Schubert, *Chem. Ber./Recueil* **1997**, *130*, 473–477.
[42] L. Valenzano, B. Civalleri, S. Chavan, S. Bordiga, M. H. Nilsen, S. Jakobsen, K. P. Lillerud, C. Lamberti, *Chem. Mater.* **2011**, *23*, 1700–1718.
[43] D. Danovich, S. Shaik, F. Neese, J. Echeverría, G. Aullón, S. Alvarez, *J. Chem. Theory Comput.* **2013**, *9*, 1977–1991.
[44] Rigaku, OD, CrysAlis PRO. Rigaku Oxford Diffraction Ltd, **2020**, Yarnton, England.
[45] G. M. Sheldrick, *Acta Cryst. Sect. C* **2015**, *71*, 3–8.
[46] O. V. Dolomanov, L. J. Bourhis, R. J. Gildea, J. A. K. Howard, H. Puschmann, *J. Appl. Crystallogr.* **2009**, *42*, 339–341.

Manuscript received: May 21, 2023
Revised manuscript received: June 24, 2023
Accepted manuscript online: June 26, 2023

